

Article

Activation and Disproportionation of Zr_2Fe Alloy as Hydrogen Storage Material

Jiangfeng Song ^{1,2} , Jingchuan Wang ², Xiaoyu Hu ³, Daqiao Meng ² and Shumao Wang ^{4,*}¹ Institute of Atomic and Molecular Physics, Sichuan University, Chengdu 610065, China; iterchina@163.com² Institute of Materials, Chinese Academy of Engineering Physics, Jianguo 621908, China; wangjingchuan@caep.cn (J.W.); mengdaqiao@caep.cn (D.M.)³ School of Resource & Environment and Safe Engineering, University of South China, Hengyang 421001, China; 13990105175@163.com⁴ Energy Materials and Technology Research Institute, General Research Institute for Nonferrous Metals, Beijing 100088, China

* Correspondence: hydrogen@grinm.com; Tel.: +86-10-82241238

Academic Editors: Takayuki Ichikawa and Ankur Jain

Received: 1 March 2019; Accepted: 12 April 2019; Published: 19 April 2019



Abstract: As a hydrogen storage material, Zr_2Fe alloy has many advantages such as fast hydrogen absorption speed, high tritium recovery efficiency, strong anti-pulverization ability, and difficulty self-igniting in air. Zr_2Fe alloy has lower hydrogen absorption pressure at room temperature than $LaNi_5$ alloy. Compared with the $ZrVFe$ alloy, the hydrogen release temperature of Zr_2Fe is lower so that the material can recover hydrogen isotopes at lower hydrogen concentration efficiently. Unfortunately, the main problem of Zr_2Fe alloy in application is that a disproportionation reaction is easy to occur after hydrogen absorption at high temperature. At present, there is little research on the generation and influencing factors of a disproportionation reaction in Zr_2Fe alloy. In this paper, the effects of temperature and hydrogen pressure on the disproportionation of Zr_2Fe alloy were studied systematically. The specific activation conditions and experimental parameters for reducing alloy disproportionation are given, which provide a reference for the specific application of Zr_2Fe alloy.

Keywords: Zr_2Fe ; activation; disproportionation; hydrogen isotope

1. Introduction

A tritium safety containment system plays an important role in the fusion reactors. The recovery of tritium from tailed helium gas is an indispensable technology for the efficient use of tritium. For the Zr-based alloy-filled flow bed in the inert gas environment, the hydrogen and its isotope absorption efficiency is extremely high, which fulfils the performance requirements as recovery materials [1–5]. In particular, Zr_2Fe alloy has the advantages of fast hydrogen absorption rate and high absorption efficiency. Compared with those of the high concentration hydrogenation materials [6–9], the equilibrium pressure at room temperature is around 10^{-6} Pa for Zr_2Fe alloy [10]. Zr_2Fe alloy has high feasibility and safety for the application of hydrogen storage and treatment. However, the Zr-based alloy is easy to disproportionate during high-temperature operation, which greatly reduces the storage capacity of the alloy, and is not conducive to repeated cycle applications. Hara et al. [11] carried out a lot of research on the hydrogen disproportionation reaction of Zr_2M series alloys, and found that Zr_2M series alloys can form stable Zr_2MH_5 ($M = Ni, Co, Fe$) hydrides. Otherwise, the alloy is prone to disproportionation. Especially when the temperature is raised to 773 K, the disproportionation reaction of this alloy proceeds very quickly, and the ZrH_2 phase is formed within minutes. At this temperature, $ZrCo$, $ZrNi$, and other alloys also disproportionate, however, the reaction rate is significantly slower.

Zr₂Fe alloy is more prone to disproportionation than other alloys. Prigent et al. [12] measured the cyclic properties of Zr₂Fe alloy at 0.10 MPa under pure hydrogen conditions. The results showed that the hydrogen absorption capacity was significantly affected by the number of cycles. When hydrogen is absorbed for the first time, the hydrogen absorption capacity is about 1.88 wt %. After hydrogen evolution at 350 °C for 3 h, the second hydrogen absorption capacity becomes 1.18 wt %. Under the same conditions, the hydrogen capacity is only 0.84 wt % after third cycle. The decreased hydrogen storage capacity can directly reflect the extent of the disproportionation reaction. Roupová et al. [13] also found that the zirconium-rich phase Zr₂Fe in the structure is more prone to disproportionation after hydrogen absorption. Temperature and pressure are the most commonly used system control parameters in applications, but are rarely reported in literature. In this paper, the activation method of Zr₂Fe alloy and the disproportionation effect of different temperature and hydrogen partial pressure on Zr₂Fe alloy were studied systematically. The specific activation parameters and the method to reduce the disproportionation of the alloy are given below.

2. Results and Discussions

2.1. Optimization of Activation Parameters of Zr₂Fe Alloy

XRD patterns of the as-received Zr₂Fe alloy without any handling are shown in Figure 1. Zr₂Fe was successfully obtained and presented a polycrystalline structure. Unfortunately, the diffraction peak of Zr₂FeO_x in powder was observed in the XRD pattern, which was the reason for activation prior to use.

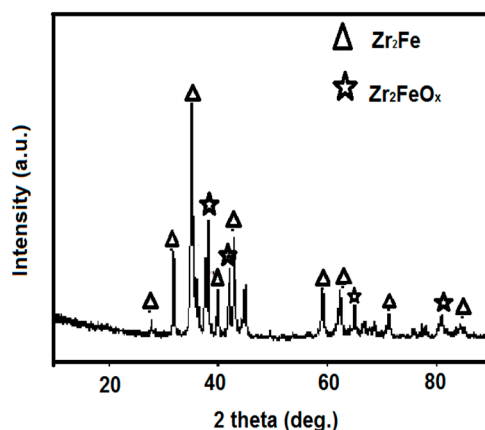


Figure 1. X-ray power diffraction (XRD) pattern of Zr₂Fe alloy.

2.1.1. Optimization of Activation Temperature

The as-received Zr₂Fe samples were firstly activated and made to form Zr₂Fe hydride under H₂ with 0.1 MPa at different temperatures (300 °C, 400 °C, and 500 °C) for 3 h. Figure 2 shows the hydrogen absorption kinetic curves for samples after activation. It can be seen that the samples at different activated conditions achieve hydrogen saturation essentially within 100 s and the most hydrogen absorption of tested samples are 1.765 wt %, 1.848 wt %, and 1.836 wt % at 300 °C, 400 °C, and 500 °C, respectively. Some interesting phenomena were discovered. It was clear that the amount of hydrogen absorption for samples handled at 400 °C and 500 °C was astonishingly greater than when activated at 300 °C, indicating that activation temperature above 400 °C was required to reach complete activation for Zr₂Fe alloy. Meanwhile, maximum hydrogen absorption and kinetic trends of samples activated under 400 °C and 500 °C is similar in Figure 2, indicating that the effects of raising temperature to 500 °C on an activated sample are weak and the Zr₂Fe alloy could be completely activated at 400 °C in a vacuum.

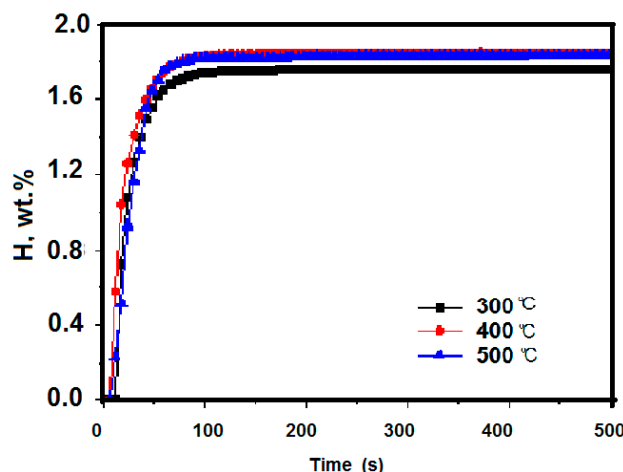


Figure 2. Kinetics of hydrogen absorption at 0.1 MPa after 3 h activation at different temperatures.

The crystal structure of activated Zr_2Fe alloy after hydrogenation at room temperature was carried out by X-ray diffraction, as shown in Figure 3. It is clear that Zr_2FeH_5 is considered a principle phase for Zr_2Fe hydride at room temperature, and a small impurity phase is also observed, such as ZrH_2 and $ZrFe_2$, indicating that a part of the Zr_2FeH_5 phase is disproportionated firstly at hydrogen absorption. The hydrogen absorption and disproportionation reaction of Zr_2Fe is shown below:

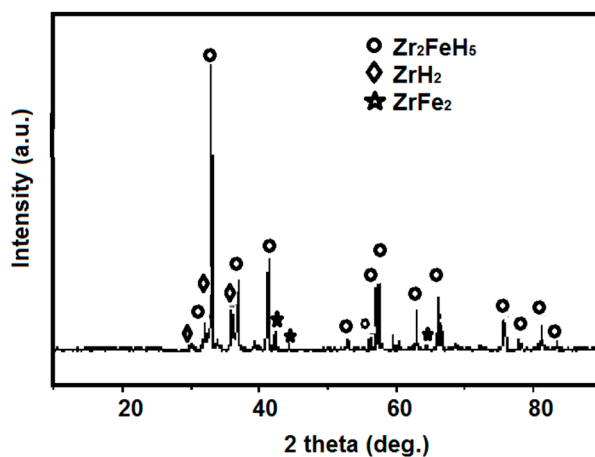
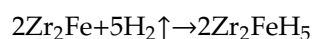


Figure 3. XRD patterns of the hydrogenated product of Zr_2Fe alloy.

2.1.2. Optimization of Activation Treatment Time

The activation temperature was taken at 400 °C and the activation time took 1 to 4 h. The corresponding room temperature hydrogen absorption kinetics curve is shown in Figure 4. The maximum hydrogen absorption of Zr_2Fe alloy after different activation treatment times was 1.707 wt %, 1.752 wt %, 1.848 wt %, and 1.840 wt %. It can be seen from Figure 5 that when activating for 1 h, the hydrogen absorption of the material had a certain incubation period. As the activation time was prolonged, the incubation period was shortened to zero, and the maximum hydrogen absorption gradually increased. When the activation time reached 3 h or more, the maximum hydrogen absorption amount was 1.84%, indicating that prolonging the activation time contributed to the activation

of the material. When the activation time reaches 3 h or more, the material can be substantially activated completely.

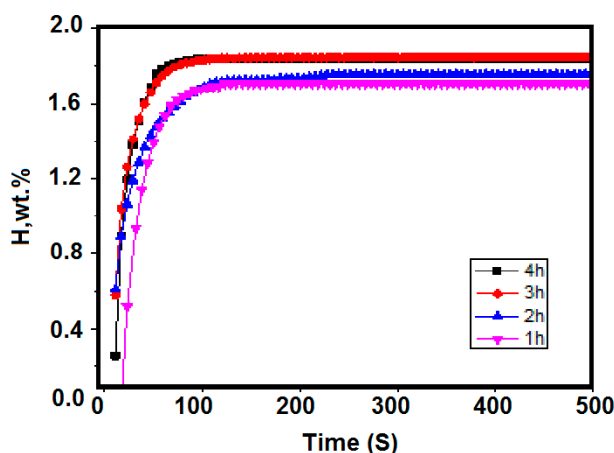


Figure 4. Hydrogen absorption kinetics curves at different activation times of 400 °C at 0.1 MPa.

2.1.3. Optimization of the Initial Activation Hydrogen Pressure

The activation time is 3 h at 400 °C, and the hydrogen absorption kinetics at room temperature under different hydrogen pressures (0.1, 0.3, 0.65 MPa) are shown in Figure 5. It can be found that as the initial hydrogen absorption pressure increased, the hydrogen absorption rate gradually increased, while the hydrogen absorption amount decreased gradually. At 0.1, 0.3, and 0.65 MPa, the maximum hydrogen absorption of the materials was 1.848 wt %, 1.406 wt %, and 1.302 wt %, respectively. It can be inferred that at higher hydrogen pressures, the material may be disproportionated.

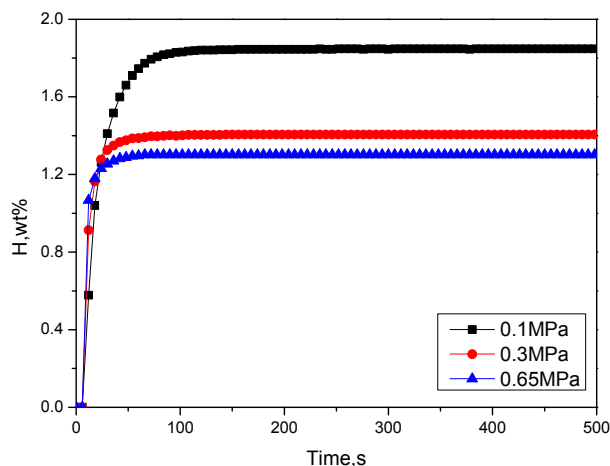


Figure 5. Hydrogen absorption kinetics curves at room temperature and different pressures after activating Zr_2Fe at 400 °C for 3 h.

By comparing the XRD patterns of the samples after hydrogen saturation at different initial hydrogen pressures as shown in Figure 6, it is found that, under the same activation temperature and time, and under a certain hydrogen pressure, the hydrogen absorption products of Zr_2Fe alloy form with Zr_2FeH_5 , ZrH_2 , $ZrFe_2$ phase composition. Among them, the hydrogen absorption product under the initial hydrogen pressure of 0.1 and 0.3 MPa is dominated by Zr_2FeH_5 , and the peak of the main phase of the sample Zr_2FeH_5 which absorbs hydrogen under a hydrogen pressure of 0.1 MPa is high, containing only a small amount of other heterophases. The sample after hydrogen absorption at initial hydrogen pressure of 0.65 MPa is mainly composed of disproportionation product phase ZrH_2 and $ZrFe_2$, as shown in the rhombic and empty rhombic shapes in the XRD patterns, respectively. The ZrH_2

and $ZrFe_2$ diffraction peaks are stronger than the sample with an initial hydrogen absorption pressure of 0.3 MPa, which means the disproportionation product is more.

Therefore, the Zr_2Fe alloy is prone to disproportionation under a certain hydrogen pressure, and the hydrogenation product Zr_2FeH_5 undergoes a disproportionation reaction, while hydrogen absorption results in the material not reaching the saturated hydrogen absorption amount.

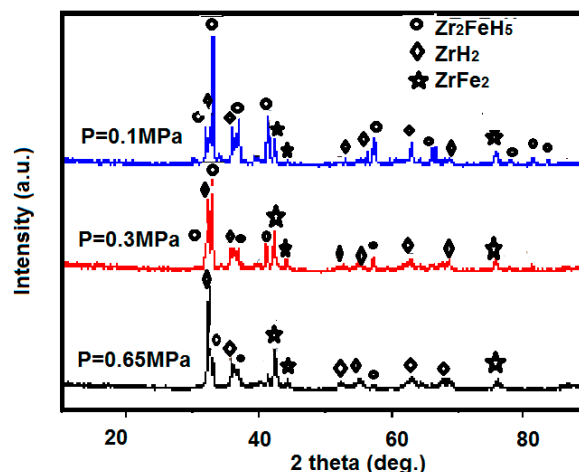


Figure 6. XRD pattern of Zr_2Fe alloy after hydrogen absorption at different initial hydrogen pressures after activation at 400 °C for 3 h.

2.2. Disproportionation Properties of Zr_2Fe Alloy

The above studies show that the initial hydrogen pressure has a significant effect on the hydrogen absorption disproportionation of the Zr_2Fe alloy. When the hydrogen absorption pressure is slightly higher, the disproportionation product phase is formed. In order to study the effect of temperature on the hydrogenation disproportionation of Zr_2Fe alloy, the experimental design of this stage is as follows: Firstly, it is activated at 400 °C for 3 h, then cooled to room temperature. Hydrogen is absorbed to saturation at 0.1 MPa hydrogen pressure, and then heated to the set temperature (300–600 °C) to study the disproportionation at different temperatures.

The experimental results are shown in Figure 7. The hydrogen absorption of the Zr_2Fe alloy sample at room temperature initially heated up from 300 to 600 °C. The absorbed hydrogen was reduced from the initial saturated state, from around 1.84 wt % to 1.525 wt %, 1.374 wt %, 1.325 wt %, and 1.285 wt %. At the same time, compared with the hydrogen absorption disproportionation curve at 300 °C, it was found that the hydrogen absorption of the final equilibrium of the sample at 400–600 °C was significantly reduced, which is related to the disproportionation reaction of Zr_2FeH_5 , in addition to the effect of temperature on the saturated hydrogen absorption of Zr_2Fe alloy. Therefore, it can be inferred that the temperature at which the disproportionation reaction of the Zr_2Fe alloy starts to occur is about 400 °C. At 300 °C, the disproportionation reaction does not substantially occur.

Figure 8 shows a kinetic curve of hydrogen absorption at 300 °C under hydrogen pressure of 0.1 MPa after activation of the alloy at 400 °C. The hydrogen absorption of the material at this temperature is 1.528 wt %, and the disproportionation performance test is 300 °C. Under these conditions, the final stable hydrogen absorption amount is similar, and it can be seen that at 300 °C, no disproportionation reaction occurred substantially.

XRD scanning of the sample at 300 °C disproportionation after hydrogen absorption at room temperature is shown in Figure 9. The main phase of Zr_2Fe alloy after the 300 °C disproportionation test is Zr_2FeH_5 , but this still contains trace amounts of disproportionation products, $ZrFe_2$ and ZrH_2 . The Zr_2FeH_5 phase can be maintained substantially at 300 °C, and most of the Zr_2FeH_5 does not undergo disproportionation. Comparative analysis of the sample structure after a disproportionation test at 500 °C and 600 °C reveals that as the temperature increases, the disproportionation product

increases. The main phase of the sample product at 600 °C changed to the ZrH₂ phase, meaning that Zr₂FeH₅ is completely disproportionate.

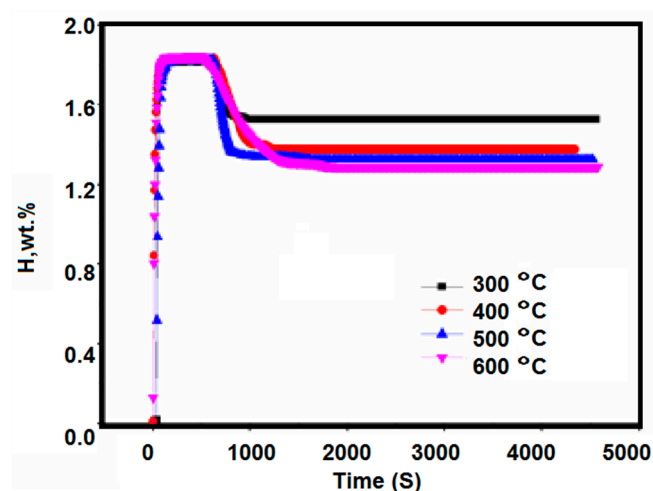


Figure 7. Disproportionation reaction curves of Zr₂FeH₅ during 1 h hydrogen release at 300–600 °C.

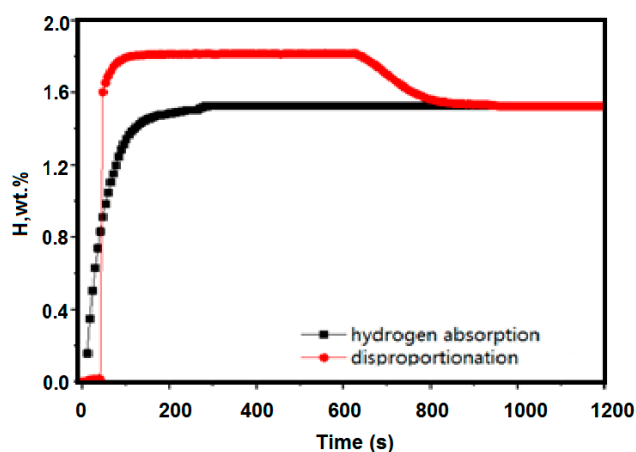


Figure 8. Kinetic curves of hydrogen absorption at 300 °C under hydrogen pressure of 0.1 MPa after activation of the alloy at 400 °C (black line); the disproportionation performance test is 300 °C (red line).

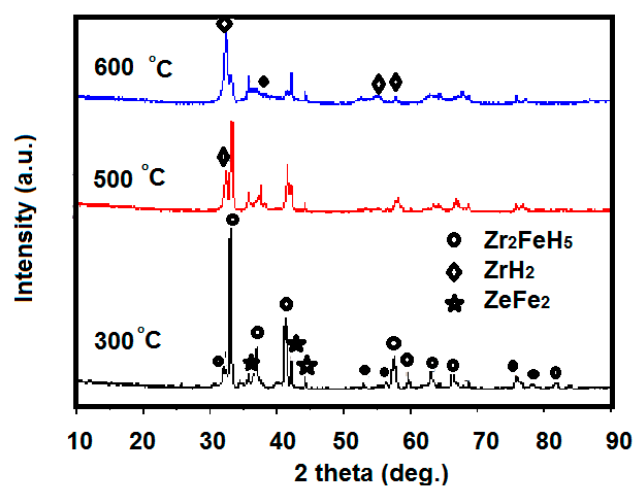


Figure 9. XRD pattern of samples after disproportionation test at different temperatures, after hydrogen absorption at room temperature.

3. Materials and Methods

The Zr_2Fe alloy was prepared by medium frequency induction melting in the form of granule, with particle size of 100–200 mesh. To test hydrogen absorption and other related properties of the alloy, 2 g samples were loaded in a homemade Sievert-type apparatus, where isothermal kinetic testing was completed on a homemade hydrogen storage material testing system, as shown in Figure 10. The dehydrogenating kinetics measurement was taken by volumetric method. All vials and valves were made of 316 L stainless steel. The furnace temperature was controlled at the accuracy of 0.5 °C. The H_2 and Ar used in measurement had a high purity of 99.99%. All the de-/hydrogenation measurements were taken in a constant environment, which was achieved by balancing the sample vial and buffer tank volume ratio. In order to avoid disproportionation and to optimize the activation process, we systematically investigated the influence of different activation conditions, especially temperature, time, and hydrogen pressure, on Zr_2Fe hydrogenation/dehydrogenation and the cooperating effect between hydrogen pressure and temperature on Zr_2Fe alloy disproportionation.

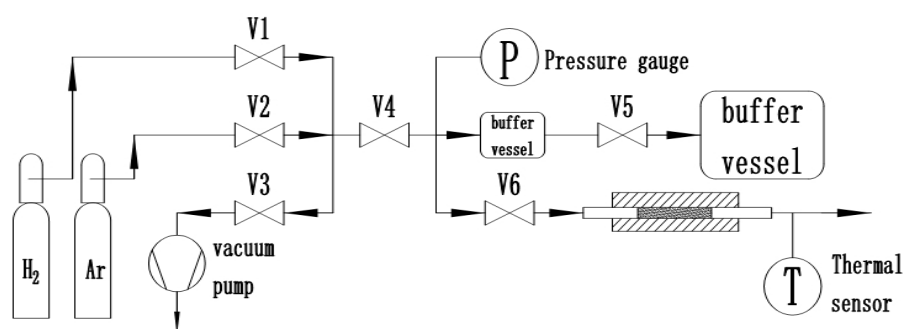


Figure 10. Hydrogen absorption and desorption performance measurement system based on Sieverts' method.

The crystal structure of the Zr_2Fe at different stages, especially hydrogen absorption and disproportionation processes, was characterized by a Smart Lab x-ray power diffraction (XRD, Rigaku, Japan) with $Cu\ K\alpha$ radiation, 45 kV, and 200 mA. Furthermore, 200 mesh powder XRD patterns were recorded in steps of 0.02° (2theta) from 10° to 90° with a constant scanning rate of $5^\circ\ min^{-1}$.

4. Conclusions

Zr_2Fe alloy is promised to be used in the tritium safety systems in future fusion reactors. In this paper, the activation process and hydrogen-induced disproportionation process of Zr_2Fe alloy were studied. The optimum activation condition of Zr_2Fe alloy is $400^\circ C$ for 3 hours. Zr_2Fe alloy is better to be used under hydrogen absorption pressure of 0.1 MPa at room temperature. The optimum hydrogenation concentration is 1.84 wt %. The hydrogen disproportionation reaction of Zr_2Fe alloy under different temperatures and pressure was also studied. The results indicate that no disproportionation reaction occurs under the condition of $300^\circ C$. The hydrogen absorption amount of Zr_2Fe alloy is 1.528 wt % at 0.1 MPa hydrogen pressure.

Author Contributions: Methodology, J.S.; resources, J.W.; data curation, S.W.; writing—original draft preparation, J.S.; writing—review and editing, X.H., J.W., and S.W.; project administration, D.M.; funding acquisition, D.M.

Funding: This research was funded by the National Magnetic Confinement Fusion Science Program, grant number 2017YFE0301502.

Conflicts of Interest: The authors declare no conflict of interest.

References

1. Raj, P.; Suryanarayana, P.; Sathyamoorthy, A.; Shashikala, K. Zr_2FeH_x system hydrided at low temperatures: Structural aspects by Mössbauer and X-ray diffraction studies. *J. Alloys Compd.* **1992**, *178*, 393–401. [[CrossRef](#)]

2. Song, J.; Wang, J.; Jiang, F.; Li, P.; Zhu, Z.; Meng, D. Experiment and Simulation on Zr_2Fe Bed for Tritium Capturing. *RSC Adv.* **2019**, *9*, 1472–1475.
3. Fukada, S.; Toyoshima, Y.; Nishikawa, M. Zr_2Fe and $Zr(Mn_{0.5}Fe_{0.5})_2$ particle beds for tritium purification and impurity removal in a fusion fuel cycle. *Fusion Eng. Des.* **2000**, *49*, 805–809. [[CrossRef](#)]
4. Fukada, S.; Tokunaga, K.; Nishikawa, M. Recovery of low-concentration hydrogen from different gas streams with Zr_2Fe particle beds. *Fusion Eng. Des.* **1997**, *36*, 471–478. [[CrossRef](#)]
5. Liger, K.; Lefebvrea, X.; Ciampichettib, A.; Aiello, A.; Ricapito, I. HCLL and HCPB coolant purification system: Design of the copper oxide bed. *Fusion Eng. Des.* **2011**, *86*, 1859–1862. [[CrossRef](#)]
6. Zhang, H.; Xia, G.; Zhang, J.; Sun, D.; Guo, Z.; Yu, X. Graphene Tailored Thermodynamics and Kinetics to Fabricate Metal Borohydride Nanoparticles with High Purity and Enhanced Reversibility. *Adv. Energy Mater.* **2018**, *8*, 1702975. [[CrossRef](#)]
7. Xia, G.; Tan, Y.; Chen, X.; Sun, D.; Guo, Z.; Liu, H.; Ouyang, L.; Zhu, M.; Yu, X. Monodisperse Magnesium Hydride Nanoparticles Uniformly Self-Assembled on Graphene. *Adv. Mater.* **2015**, *27*, 5981. [[CrossRef](#)] [[PubMed](#)]
8. Huang, Y.Q.; Xia, G.L.; Zhang, J.; Guo, Z.; Yu, X. Graphene-tailored molecular bonds for advanced hydrogen and lithium storage performance. *Energy Storage Mater.* **2019**, *17*, 178. [[CrossRef](#)]
9. Xia, G.; Tan, Y.; Wu, F.; Fang, F.; Sun, D.; Guo, Z.; Huang, Z.; Yu, X. Graphene-wrapped reversible reaction for advanced hydrogen storage. *Nano Energy* **2016**, *26*, 488. [[CrossRef](#)]
10. Coleman, M.; Chandra, D.; Wermer, J. *Advanced Materials for Energy Conservation II, TMs*; The Minerals, Metals and Materials Society: Pittsburgh, PA, USA, 2004; pp. 429–435.
11. Hara, M.; Hayakawa, R.; Kaneko, Y.; Watanabe, K. Hydrogen-induced disproportionation of Zr_2M ($M=Fe, Co, Ni$) and repropotionation. *J. Alloys Compd.* **2003**, *352*, 218–225. [[CrossRef](#)]
12. Prigent, J.; Latroche, M.; Leoni, E.; Rohr, V. Hydrogen trapping properties of Zr-based intermetallic compounds in the presence of CO contaminant gas. *J. Alloys Compd.* **2011**, *509*, 801–803. [[CrossRef](#)]
13. Roupová, P.; Schneeweiss, O.; Zhu, M. Hydrogenation of nanocrystalline Zr-Fe-H powder. *J. Alloys Compd.* **2005**, *404*, 537–540. [[CrossRef](#)]

Sample Availability: Samples of the compounds are not available from the authors.



© 2019 by the authors. Licensee MDPI, Basel, Switzerland. This article is an open access article distributed under the terms and conditions of the Creative Commons Attribution (CC BY) license (<http://creativecommons.org/licenses/by/4.0/>).